Structural Engineering and Mechanics, *Vol. 69, No. 5 (2019) 527-536*
DOI: https://doi.org/10.12989/sem.2019.69.5.527

Theoretical equivalence and numerical performance of T3γ_s and MITC3 plate finite elements

Andi Makarim Katili, Imam Jauhari Maknun and Irwan Katili*

Department of Civil Engineering, Universitas Indonesia, Depok 16424, Indonesia

(Received June 14, 2018, Revised January 18, 2019, Accepted January 23, 2019)

Abstract. This paper will compare T3γ_s and MITC3 elements, both these two elements are three-node triangular plate bending elements with three degrees of freedom per node. The formulation of the T3γ_s and MITC3 elements is rather simple and has already been widely used. This paper will prove that the shear strain formulation of these two elements is identical even though they are obtained from two different methods. A single element is used to test the formulation of shear strain matrices. Numerical tests for circular plate cases compared with the exact solutions and with DKMT element will complete this review to verify the performances and show the convergence of these two elements.

Keywords: plate bending element; T3γ_s; MITC3; Reissner-Mindlin plate theory; assumed natural strain

1. Introduction

The challenge of the finite element is how to generate a simple and applicable element formulation to reduce the computational cost, yet providing high accuracy and good convergence. In structural modeling, the use of a triangular element is interesting due to the simplicity and flexibility. Three node triangular elements are mostly used for complex configurations. However, research on triangular elements is not so intensive compared to the quadrilateral element. Hence, many analysts prefer to use quadrilateral element (Katili *et al*. 2014, 2015, 2018), Mahjudin *et al.* (2016) and Maknun *et al*. (2016), Wong *et al.* (2017), Ko *et al.* (2017) and Banh and Lee (2018). This situation should encourage researchers to develop low order triangular element.

Formulation of plate element based on Reissner-Mindlin theory with C^0 continuity results in shear locking phenomenon, which is responsible for giving poor results in thin plate problems, at least with low order approximation. To deal with this phenomenon, reduced and selective integration have been used to improve the performance of elements, but the shear locking cannot always be overcome.

Mixed formulation and Assumed Natural Strain (ANS) have been better alternatives to overcome the problem of shear locking was proposed by Hughes and Tezduyar (1981) and MacNeal (1982). ANS has been found a very effective method used by many authors to develop new finite elements based on Reissner-Mindlin plate theory.

One of the simplest ANS formulation to obtain a 3 nodes, three degrees of freedom (dof) per node, plate bending element with Transverse Shear (TS) effects included is due to Hughes and Taylor (1982). They consisted in two things: the first was to express the transverse shear strains in terms of the three constant tangential shear strains on each side which are then expressed in terms of the nodal variables. This was an application of what is now called the Assumed Natural Strain (ANS) or independent transverse shear approach. Another paper using the same formulation called TCSS (Triangular with Constant Shear on Sides) element was presented by Ayad *et al*. in 1992. In this present paper this element, called as T3γ_s, has a constant TS at sides of the element and uses the shear projection method to obtain TS on nodes.

DKT (Discrete Kirchhoff Triangular) element, proposed by Batoz, Bathe and Ho in 1980, was developed based on the Reissner-Mindlin theory but using discrete Kirchhoff constraints on edges to neglect Transverse Shear (TS) energy. This element passes the patch test and gives good performance but it is only valid for thin plate cases.

Based on the DKT element Batoz and Lardeur (1989) proposed the triangular element called DST (Discrete Shear Triangular), where TS effects have been considered using element equilibrium equations and shear constitutive equations to define constant shear strains along the three edges of the element. DST element give overall good behavior for the analysis of thin to thick plates but the transverse shear contribution is a bit complicated and patch tests for very thick plates were not fully satisfied.

Combining several aspects of the formulation of DKT, T3γ_s and DST, Katili (1993) proposed DKMT (Discrete Kirchoff Mindlin Triangular) element using simplified equilibrium equation for assumed constant transverse shear strains along element sides. DKMT is valid for thin to thick plates, has good convergence properties and fully satisfies patch tests. DKMT element is free of shear locking by element constructions since as DKMT converges to DKT for thin plates.

The MITC3, triangular shell element proposed by Lee

∗Corresponding author, Professor
E-mail: irwan.katili@eng.ui.ac.id

http://www.techno-press.com/journals/sem&subpage=7 ISSN: 1225-4568 (Print), 1598-6217 (Online)

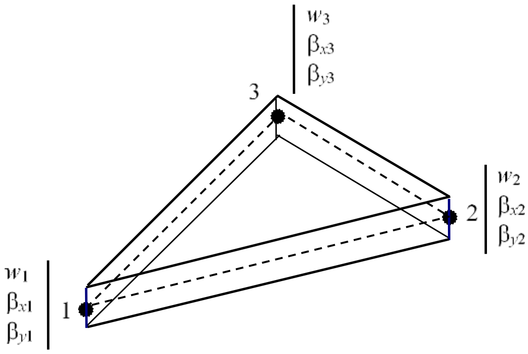

Fig. 1 Triangular element and degrees of freedom

and Bathe (2004), is another popular triangular element with several of studies and developments (Lee *et al*. 2007) and (Lee *et al*. 2012). This 3-node triangular element has a simple and general formulation. The improvement of MITC3 shell elements called MITC3+ has been recently proposed by Jeon *et al.* (2015) and Ko *et al.* (2017).

The purpose of this paper is to compare the formulation and performance of the two triangular elements, T3γ_s and MITC3, and compare the numerical results of both elements with DKMT element. The paper is organized as follows. Some aspects of the formulation of T3γ_s are recalled in section 2. In sections 3 and 4, the formulation of DKMT and MITC3 is presented using the same notation as for the formulation of T3γ_s. Section 5 deals with the numerical tests for circular plate problems to evaluate the convergence of both elements and compare the results with DKMT element. Concluding remarks, acknowledgments and references are given at the end.

2. Formulation of the T3γ_s element

One of the developments for plate bending elements proposed by Hughes and Taylor (1982) for the triangular element is called in this paper as T3γ_s, is generated by an assumed natural strain concept. Transversal shear strain for this element is expressed with special interpolation called shear projection method. The triangular elements discussed here have three-degrees of freedom per node (Fig. 1).

2.1 Bending strain matrix

The displacement functions are given as

$$w=\sum_{i=1}^{3} N_i\, w_i \quad ; \quad \beta_x=\sum_{i=1}^{3} N_i\, \beta_{x_i} \quad ; \quad \beta_y=\sum_{i=1}^{3} N_i\, \beta_{y_i} \tag{1}$$

where:

w is the vertical displacement function

β_x and β_y are the rotations in plane of z-x and z-y, respectively.

N_i is a shape function and the shape functions are

$$N_1=1-\xi-\eta \quad ; \quad N_2=\xi \quad ; \quad N_3=\eta \tag{2}$$

The relation between curvature and rotation is declared as

$$\{\chi\}=\begin{Bmatrix}\chi_x\\ \chi_y\\ \chi_{xy}\end{Bmatrix}=\begin{Bmatrix}\beta_{x,x}\\ \beta_{y,y}\\ \beta_{x,y}+\beta_{y,x}\end{Bmatrix} \tag{3}$$

$\beta_{x,x}$ and $\beta_{x,y}$ denote the first derivatives of β_x with respect to x and y, respectively.

The relation between curvature and nodal displacement is expressed in the equation

$$\{\chi\}=[B_b]\{u_n\} \tag{4}$$

$\{u_n\}$: Nodal displacements

$$\{u_n\}=\langle u_n\rangle^T=\langle \ldots \quad w_i \quad \beta_{x_i} \quad \beta_{y_i} \quad \ldots\rangle^T_{i=1,2,3} \tag{5}$$

$[B_b]$: From Eqs. (1)-(4), we obtain the expression of the bending strain matrix,

$$[B_b]=\begin{bmatrix} & 0 & N_{i,x} & 0 & \\ \ldots & 0 & 0 & N_{i,y} & \ldots \\ & 0 & N_{i,y} & N_{i,x} & \end{bmatrix}_{i=1,2,3} \tag{6}$$

$N_{i,x}$ and $N_{i,y}$ denote the first derivatives of N_i with respect to x and y, respectively.

$$\begin{Bmatrix}N_{i,x}\\ N_{i,y}\end{Bmatrix}=[j]\begin{Bmatrix}N_{i,\xi}\\ N_{i,\eta}\end{Bmatrix} \tag{7}$$

where $[j]$ is the inverse of Jacobian matrix, and the Jacobian matrix is

$$[J]=\begin{bmatrix}J_{11} & J_{12}\\ J_{21} & J_{22}\end{bmatrix}=\begin{bmatrix}x_{,\xi} & y_{,\xi}\\ x_{,\eta} & y_{,\eta}\end{bmatrix}=\begin{bmatrix}x_{21} & y_{21}\\ -x_{13} & -y_{13}\end{bmatrix} \tag{8}$$

$$x_{ji}=x_j-x_i \ ; \ y_{ji}=y_j-y_i$$

The inverse of Jacobian is

$$[j]=\begin{bmatrix}j_{11} & j_{12}\\ j_{21} & j_{22}\end{bmatrix}=\frac{1}{2A}\begin{bmatrix}-y_{13} & -y_{21}\\ x_{13} & x_{21}\end{bmatrix} \tag{9}$$

$$\det[J]=2A \ ; \ A \text{ is the area of the element}$$

From Eqs. (5)-(9), we obtain the expression of the bending strain matrix as

$$[B_b]=\frac{1}{2A}\begin{bmatrix}0 & -y_{32} & 0 & 0 & -y_{13} & 0 & 0 & -y_{21} & 0\\ 0 & 0 & x_{32} & 0 & 0 & x_{13} & 0 & 0 & x_{21}\\ 0 & x_{32} & -y_{32} & 0 & x_{13} & -y_{13} & 0 & x_{21} & -y_{21}\end{bmatrix} \tag{10}$$

2.2 Shear strain interpolation

The shear strain field is assumed linear in each element

$$\{\underline{\gamma}\}=\begin{Bmatrix}\underline{\gamma}_x\\ \underline{\gamma}_y\end{Bmatrix}=\sum_{i=1}^{3} N_i\begin{Bmatrix}\underline{\gamma}_{x_i}\\ \underline{\gamma}_{y_i}\end{Bmatrix} \tag{11}$$

where: $\underline{\gamma}_{x_i}$ and $\underline{\gamma}_{y_i}$ are the shear strains at node-*i*

Shear strain is assumed constant along sides of the element (Fig. 2). Shear strain at node–*i* is obtained from the projection of constant shear strain $\underline{\gamma}_{s_{ij}}$ from each side of the element to the nodes of the element.

$$\begin{Bmatrix} \underline{\gamma}_{s_{12}} \\ \underline{\gamma}_{s_{31}} \end{Bmatrix} = \begin{bmatrix} C_{12} & S_{12} \\ C_{31} & S_{31} \end{bmatrix} \begin{Bmatrix} \underline{\gamma}_{x_1} \\ \underline{\gamma}_{y_1} \end{Bmatrix}$$
$$\begin{Bmatrix} \underline{\gamma}_{s_{23}} \\ \underline{\gamma}_{s_{12}} \end{Bmatrix} = \begin{bmatrix} C_{23} & S_{23} \\ C_{12} & S_{12} \end{bmatrix} \begin{Bmatrix} \underline{\gamma}_{x_2} \\ \underline{\gamma}_{y_2} \end{Bmatrix} \quad (12)$$
$$\begin{Bmatrix} \underline{\gamma}_{s_{31}} \\ \underline{\gamma}_{s_{23}} \end{Bmatrix} = \begin{bmatrix} C_{31} & S_{31} \\ C_{23} & S_{23} \end{bmatrix} \begin{Bmatrix} \underline{\gamma}_{x_3} \\ \underline{\gamma}_{y_3} \end{Bmatrix}$$

where

$$C_{ij} = \frac{x_{ji}}{L_{ij}} \;;\; S_{ij} = \frac{y_{ji}}{L_{ij}} \;;\; L_{ij} = \sqrt{x_{ji}^2 + y_{ji}^2} \quad (13)$$

From Eqs. (11)-(13), we obtain

$$\{\underline{\gamma}\} = \begin{Bmatrix} \underline{\gamma}_x \\ \underline{\gamma}_y \end{Bmatrix} = \left[B_{s_\gamma} \right] \{\underline{\gamma}_{s_n}\} \quad (14)$$

with

$$\left[B_{s_\gamma} \right] = \begin{bmatrix} \left(\frac{S_{31}}{A_1} N_1 - \frac{S_{23}}{A_2} N_2 \right) & \left(\frac{S_{12}}{A_2} N_2 - \frac{S_{31}}{A_3} N_3 \right) & \left(\frac{S_{23}}{A_3} N_3 - \frac{S_{12}}{A_1} N_1 \right) \\ -\left(\frac{C_{31}}{A_1} N_1 - \frac{C_{23}}{A_2} N_2 \right) & -\left(\frac{C_{12}}{A_2} N_2 - \frac{C_{31}}{A_3} N_3 \right) & -\left(\frac{C_{23}}{A_3} N_3 - \frac{C_{12}}{A_1} N_1 \right) \end{bmatrix} \quad (15)$$

and

$$\begin{aligned} A_1 &= C_{12}\, S_{31} - C_{31}\, S_{12} \\ A_2 &= C_{23}\, S_{12} - C_{12}\, S_{23} \\ A_3 &= C_{31}\, S_{23} - C_{23}\, S_{31} \end{aligned} \quad (16)$$

$$\left\{ \underline{\gamma}_{s_n} \right\} = \left\langle \underline{\gamma}_{s_n} \right\rangle^T = \left\langle \underline{\gamma}_{s_{12}} \quad \underline{\gamma}_{s_{23}} \quad \underline{\gamma}_{s_{31}} \right\rangle^T \quad (17)$$

If the assumed shear force and shear strains are constant along the side, then we obtain

$$\underline{\gamma}_{s_{ij}} = \frac{1}{L_{ij}} \int_0^{L_{ij}} \gamma_s \, ds \quad (18)$$

On each side *i-j*, we recall that *w*, β_x and β_y have a linear variation in *s*

$$\begin{aligned} \gamma_s &= w,_s + \beta_s \\ w &= \left(1 - \frac{s}{L_{ij}} \right) w_i + \frac{s}{L_{ij}} w_j \\ \beta_s &= \left(1 - \frac{s}{L_{ij}} \right) \beta_{s_i} + \frac{s}{L_{ij}} \beta_{s_j} \end{aligned} \quad (19)$$

Using Eqs. (18)-(19), we obtain

$$\begin{aligned} \underline{\gamma}_{s_{ij}} &= \frac{1}{L_{ij}} \left(w_j - w_i \right) + \frac{1}{2} \beta_{s_i} + \frac{1}{2} \beta_{s_j} \\ \underline{\gamma}_{s_{ij}} &= \frac{1}{L_{ij}} \left(w_j - w_i \right) + \frac{1}{2} \left(C_{ij} \beta_{x_i} + S_{ij} \beta_{y_i} + C_{ij} \beta_{x_j} + S_{ij} \beta_{y_j} \right) \end{aligned} \quad (20)$$

Using Eq. (20) for all sides we get

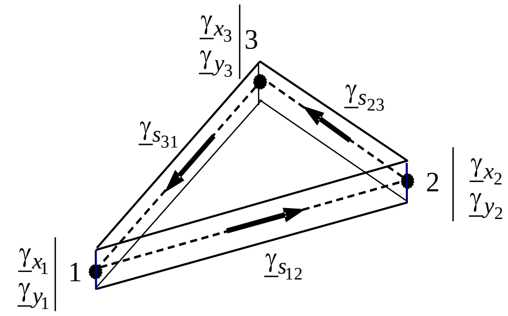

Fig. 2 Constant transverse shear strain along the side *ij* for T3γ_s

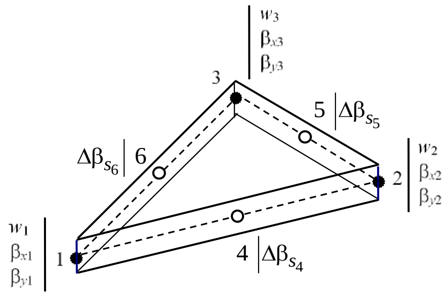

i	*j*	*k*
1	2	4
2	3	5
3	1	6

Fig. 3 DKMT element, corner and temporary degrees of freedom at mid side of the element

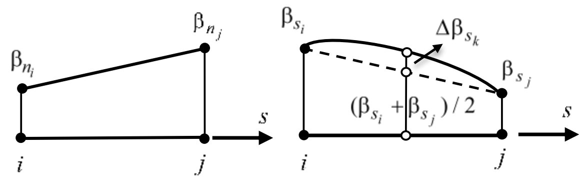

Fig. 4 Rotations β_s and β_n on each side *i-j* of an element.

$$\{\underline{\gamma}_{s_n}\} = [A_u]\{u_n\} \quad (21)$$

Where $[A_u]$ is

$$[A_u] = \frac{1}{2} \begin{bmatrix} -\frac{2}{L_{12}} & C_{12} & S_{12} & \frac{2}{L_{12}} & C_{12} & S_{12} & 0 & 0 & 0 \\ 0 & 0 & 0 & -\frac{2}{L_{23}} & C_{23} & S_{23} & \frac{2}{L_{23}} & C_{23} & S_{23} \\ \frac{2}{L_{31}} & C_{31} & S_{31} & 0 & 0 & 0 & -\frac{2}{L_{31}} & C_{31} & S_{31} \end{bmatrix} \quad (22)$$

Introducing Eqs. (21)-(22) into Eq. (14) we have

$$\{\underline{\gamma}\} = \begin{Bmatrix} \underline{\gamma}_x \\ \underline{\gamma}_y \end{Bmatrix} = [B_s]\{u_n\} \;;\; [B_s] = \left[B_{s_\gamma} \right][A_u] \quad (23)$$

The shear stiffness for T3γ_s is calculated using three-points of Hammer integration.

3. Formulation of DKMT element

The DKMT element first published by Katili (1993) combines some ideas and formulation aspects found in DKT, DST and T3γ_s to achieve a simple and efficient element valid for thin to thick plates. DKMT element has 3 nodes with 3 degrees of freedom each, which are: w (translation in the z-direction), β_x (rotation in the z-x plane) and β_y (rotation in the z-y plane). Incomplete quadratic rotation fields for β_x and β_y are considered in terms of rotations at the three corners and a temporary variable at mid-side i-j (Fig. 3).

On each side i-j, the normal rotation β_n is a linear function of s, while rotation β_s is quadratic in s (Fig. 4).

In a hierarchical form

$$\beta_n = \left(1 - \frac{s}{L_k}\right)\beta_{n_i} + \frac{s}{L_k}\beta_{n_j} \tag{24}$$

$$\beta_s = \left(1 - \frac{s}{L_k}\right)\beta_{s_i} + \left(\frac{s}{L_k}\right)\beta_{s_j} + 4\frac{s}{L_k}\left(1 - \frac{s}{L_k}\right)\Delta\beta_{s_k} \tag{25}$$

The displacement function is given as

$$\begin{aligned} w &= \sum_{i=1}^{3} N_i\, w_i \\ \beta_x &= \sum_{i=1}^{3} N_i \beta_{x_i} + \sum_{k=4}^{6} P_k C_k \Delta\beta_{s_k} \\ \beta_y &= \sum_{i=1}^{3} N_i \beta_{y_i} + \sum_{k=4}^{6} P_k S_k \Delta\beta_{s_k} \end{aligned} \tag{26}$$

where: P_k are the quadratic functions

$$P_4 = 4\lambda\xi \quad ; \quad P_5 = 4\xi\eta \quad ; \quad P_6 = 4\lambda\eta \tag{27}$$

C_k and S_k are the cosinus and sinus directions and L_k is the length of side-k of the element

$$\begin{aligned} C_4 = C_{12} \quad &; \quad C_5 = C_{23} \quad ; \quad C_6 = C_{31} \\ S_4 = S_{12} \quad &; \quad S_5 = S_{23} \quad ; \quad S_6 = S_{31} \\ L_4 = L_{12} \quad &; \quad L_5 = L_{23} \quad ; \quad L_6 = L_{31} \end{aligned} \tag{28}$$

The relation between curvature and nodal displacement is expressed in the equation below.

$$\{\chi\} = \left[B_{b_\beta}\right]\{u_n\} + \left[B_{b_{\Delta\beta}}\right]\left\{\Delta\beta_{s_n}\right\} \tag{29}$$

The bending strain $\left[B_{b_\beta}\right]$ is the same as $[B_b]$ for T3γ_s, (see Eq. (10))

where

$$\left\{\Delta\beta_{s_n}\right\} = \left\langle\Delta\beta_{s_n}\right\rangle^T = \left\langle\Delta\beta_{s_4} \quad \Delta\beta_{s_5} \quad \Delta\beta_{s_6}\right\rangle^T \tag{30}$$

$$\left[B_{b_{\Delta\beta}}\right] = \begin{bmatrix} & P_{k,x}\, C_k & \\ \ldots & P_{k,y}\, S_k & \ldots \\ & P_{k,y}\, C_k + P_{k,x}\, S_k & \end{bmatrix}_{k=4,5,6} \tag{31}$$

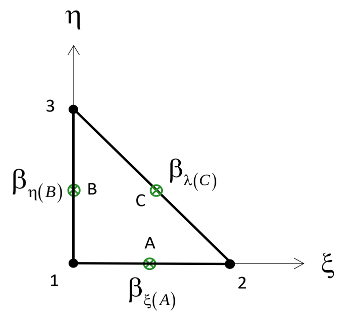

Fig. 5 Tying points

$P_{k,x}$ and $P_{k,y}$ denote the first derivatives of P_k with respect to x and y, respectively.

The assumed TS strain field is similar compared to T3γ_s, (see Eqs. (11)-17)). The independent transverse shear strains are using local equilibrium and constitutive equations considering each side as a beam in order to keep the C^0 continuity.

In 1993, Katili proposed the assumed independent transverse shear strain $\underline{\gamma}_s$ along the side i-j, can be expressed as

$$\underline{\gamma}_{s_{ij}} = \underline{\gamma}_{s_k} = -\frac{2}{3}\phi_k \Delta\beta_{s_k} \quad ; \quad \phi_k = \frac{2}{\kappa(1-\upsilon)}\left(\frac{h^2}{L_k^2}\right) \tag{32}$$

where κ is the shear correction factor (usually $\kappa = 5/6$),

The factor ϕ_k, which is characterizing the influence of shear effects, maintains the consistency of proposed element and precisely explains why DKMQ element behaves as either the *Reissner-Mindlin* theory for a thick plate or as *Kirchhoff-Love* theory for the thin plate. In the thin plate problems, where factor ϕ_k is close to zero, shear strain is automatically reduced. Accordingly, as the main positive result, the *shear locking* is automatically resolved by this Discrete Kirchhoff Mindlin method. If Eq. (32) is applied to all sides of the element, the following matrix relation is obtained

$$\begin{aligned} \left\{\underline{\gamma}_{s_n}\right\} &= \left[A_\phi\right]\left\{\Delta\beta_{s_n}\right\} \\ \left\{\underline{\gamma}_{s_n}\right\} &= \left\langle\underline{\gamma}_{s_n}\right\rangle^T = \left\langle\underline{\gamma}_{s_4} \quad \underline{\gamma}_{s_5} \quad \underline{\gamma}_{s_6}\right\rangle^T \end{aligned} \tag{33}$$

$$\left[A_\phi\right] = -\frac{2}{3}\begin{bmatrix} \phi_4 & 0 & 0 \\ 0 & \phi_5 & 0 \\ 0 & 0 & \phi_6 \end{bmatrix} \tag{34}$$

Introducing (33) into (14), the shear strains for DKMQ can be expressed as

$$\{\underline{\gamma}\} = \begin{Bmatrix} \underline{\gamma}_x \\ \underline{\gamma}_y \end{Bmatrix} = \left[B_{s_\gamma}\right]\left[A_\phi\right]\left\{\Delta\beta_{s_n}\right\} \tag{35}$$

Combining Eqs. (18), (32) and (19) with β_s in Eq. (25), we obtain on each side

$$-\frac{2}{3}\left(1+\phi_k\right)\Delta\beta_{s_k} = \frac{w_j-w_i}{L_k}+\frac{1}{2}\left(C_k\beta_{x_i}+S_k\beta_{y_i}+C_k\beta_{x_j}+S_k\beta_{y_j}\right) \quad (36)$$

Applying Eq. (36) to all sides of the element, we get

$$\left\{\Delta\beta_{s_n}\right\}=\left[A_\Delta\right]^{-1}\left[A_u\right]\left\{u_n\right\} \quad (37)$$

with

$$\left[A_\Delta\right]=-\frac{2}{3}\begin{bmatrix}(1+\phi_4) & 0 & 0\\ 0 & (1+\phi_5) & 0\\ 0 & 0 & (1+\phi_6)\end{bmatrix} \quad (38)$$

and $[A_u]$ given by (22).

Introduction of (37) into (29) we obtain the bending curvatures for DKMT element

$$\begin{aligned}&\{\chi\}=\left[B_b\right]\{u_n\} \quad \text{where}\\ &\left[B_b\right]=\left[B_{b_\beta}\right]+\left[B_{b_{\Delta\beta}}\right]\left[A_\Delta\right]^{-1}\left[A_u\right]\end{aligned} \quad (39)$$

Introducing (37) into (35) leads to

$$\begin{aligned}&\{\underline{\gamma}\}=\left[B_s\right]\{u_n\} \quad \text{where}\\ &\left[B_s\right]=\left[B_{s_\gamma}\right]\left[A_{\phi\Delta}\right]\left[A_u\right]\end{aligned} \quad (40)$$

where

$$\left[A_{\phi\Delta}\right]=\left[A_\phi\right]\left[A_\Delta\right]^{-1}=\begin{bmatrix}\dfrac{\phi_4}{(1+\phi_4)} & 0 & 0\\ 0 & \dfrac{\phi_5}{(1+\phi_5)} & 0\\ 0 & 0 & \dfrac{\phi_6}{(1+\phi_6)}\end{bmatrix} \quad (41)$$

The bending and shear stiffness for DKMT element is calculated using three-points of Hammer integration (Katili 1993). In case the size element is very small compare to the thickness ($L_k << h$), then $[A_{\phi\Delta}] = [I]$ and $[A_\phi]^{-1} = [0]$, then the DKMT≈T3γ_s.

4. Formulation of MITC3 element

In this section, we briefly review the formulations of a 3-node triangular MITC3 proposed by Lee and Bathe (2004). This element has been developed using Mixed Interpolation of Tensorial Components initially proposed by Dvorkin and Bathe (1984).

The key to MITC3 element is the use of appropriate assumed strain interpolation and the proper choice of tying points to relate displacement interpolation and strain interpolation, which is done separately. MITC3 has the same bending strain matrix formula as T3γ_s since there is no specific formulation that makes the difference. We will describe the strain interpolation method to obtain the shear strain matrix of MITC3.

For MITC3, tying points are chosen in the mid-points (Fig. 5) of the sides 1-2, 1-3, and 2-3. Distribution of β_ξ is assumed constant along ξ direction and β_η is assumed constant along η

$$\begin{aligned}\beta_\xi &= a_1 + a_2\,\eta\\ \beta_\eta &= b_1 + b_2\,\xi\\ \beta_\lambda &= \frac{1}{\sqrt{2}}\left(\beta_\xi-\beta_\eta\right)\end{aligned} \quad (42)$$

From Eq. (42), we obtain the values of β_ξ, β_η, β_λ at the tying points *A*, *B*, and *C*.

- At point *A* (η=0): we obtain $a_1=\beta_{\xi(A)}$.
- At point *B* (ξ=0): we obtain $b_1=\beta_{\eta(B)}$.
- At node 2 (ξ=1,η=0): we obtain $\beta_\lambda(1,0)=\frac{1}{\sqrt{2}}\left(\beta_\xi(1,0)-\beta_\eta(1,0)\right)$
- At node 3 (ξ=0,η=1): we obtain $\beta_\lambda(0,1)=\frac{1}{\sqrt{2}}\left(\beta_\xi(0,1)-\beta_\eta(0,1)\right)$
- Along edge 2-3, $\beta_\lambda(1,0)=\beta_\lambda(0,1)$ leads to

$$\frac{1}{\sqrt{2}}\left(\beta_\xi(1,0)-\beta_\eta(1,0)\right)=\frac{1}{\sqrt{2}}\left(\beta_\xi(0,1)-\beta_\eta(0,1)\right)$$

Gives: $a_2=-b_2=c$. Then, Eq. (42) becomes

$$\beta_\xi=\beta_{\xi(A)}+c\eta \;\; ; \;\; \beta_\eta=\beta_{\eta(B)}-c\xi \quad (43)$$

- At point *C* (ξ=1/2,η=1/2)

$$\beta_{\lambda(C)}=\frac{1}{\sqrt{2}}\left\{\beta_{\xi(C)}-\beta_{\eta(C)}\right\} \text{ and } \beta_{\lambda(C)}=\frac{1}{\sqrt{2}}\left\{\left(\beta_{\xi(A)}+\frac{1}{2}c\right)-\left(\beta_{\eta(B)}-\frac{1}{2}c\right)\right\}$$

and we obtain the value of c

$$c=\beta_{\eta(B)}-\beta_{\xi(A)}+\beta_{\xi(C)}-\beta_{\eta(C)} \quad (44)$$

Introducing Eq. (44) into Eq. (43), we obtain the expression

$$\begin{aligned}\beta_\xi&=\beta_{\xi(A)}+\left(\beta_{\eta(B)}-\beta_{\xi(A)}+\beta_{\xi(C)}-\beta_{\eta(C)}\right)\eta\\ \beta_\eta&=\beta_{\eta(B)}-\left(\beta_{\eta(B)}-\beta_{\xi(A)}+\beta_{\xi(C)}-\beta_{\eta(C)}\right)\xi\end{aligned} \quad (45)$$

β_ξ and β_η at tying points are the average values on their sides, hence

$$\begin{aligned}\beta_{\xi(A)}&=\frac{1}{2}\left(\beta_{\xi_1}+\beta_{\xi_2}\right)\\ \beta_{\eta(B)}&=\frac{1}{2}\left(\beta_{\eta_1}+\beta_{\eta_3}\right)\\ \beta_{\xi(C)}&=\frac{1}{2}\left(\beta_{\xi_2}+\beta_{\xi_3}\right)\\ \beta_{\eta(C)}&=\frac{1}{2}\left(\beta_{\eta_2}+\beta_{\eta_3}\right)\end{aligned} \quad (46)$$

Introducing (46) into (45), we obtain

$$\begin{Bmatrix} \beta_\xi \\ \beta_\eta \end{Bmatrix} = \begin{Bmatrix} \frac{1}{2}\left(\beta_{\xi_1} + \beta_{\xi_2}\right) + \left(\frac{1}{2}\left(\beta_{\xi_2} + \beta_{\xi_3}\right) - \frac{1}{2}\left(\beta_{\eta_2} + \beta_{\eta_3}\right) - \frac{1}{2}\left(\beta_{\xi_1} + \beta_{\xi_2}\right) + \frac{1}{2}\left(\beta_{\eta_1} + \beta_{\eta_3}\right)\right)\eta \\ \frac{1}{2}\left(\beta_{\eta_1} + \beta_{\eta_3}\right) - \left(\frac{1}{2}\left(\beta_{\xi_2} + \beta_{\xi_3}\right) - \frac{1}{2}\left(\beta_{\eta_2} + \beta_{\eta_3}\right) - \frac{1}{2}\left(\beta_{\xi_1} + \beta_{\xi_2}\right) + \frac{1}{2}\left(\beta_{\eta_1} + \beta_{\eta_3}\right)\right)\xi \end{Bmatrix} \tag{47}$$

The transformation for the rotation at each node in parametric system into Cartesian system can be obtained by

$$\begin{Bmatrix} \beta_{\xi_i} \\ \beta_{\eta_i} \end{Bmatrix} = [J] \begin{Bmatrix} \beta_{x_i} \\ \beta_{y_i} \end{Bmatrix} \tag{48}$$

Substituting (48) into (47), we obtain

$$\begin{Bmatrix} \beta_\xi \\ \beta_\eta \end{Bmatrix} = \left[B_\beta\right]\{\beta_n\} \tag{49}$$

where

$$\left[B_\beta\right] = \frac{1}{2}\begin{bmatrix} \left(x_{21} + x_{32}\,\eta\right) & \left(y_{21} + y_{32}\,\eta\right) & \left(x_{21} + x_{13}\,\eta\right) & \left(y_{21} + y_{13}\,\eta\right) & x_{21}\,\eta & y_{21}\,\eta \\ -\left(x_{13} + x_{32}\,\xi\right) & -\left(y_{13} + y_{32}\,\xi\right) & -x_{13}\,\xi & -y_{13}\,\xi & -\left(x_{13} + x_{21}\,\xi\right) & -\left(y_{13} + y_{21}\,\xi\right) \end{bmatrix} \tag{50}$$

and

$$\{\beta_n\} = \langle\beta_n\rangle^T = \langle \beta_{x_1} \quad \beta_{y_1} \quad \beta_{x_2} \quad \beta_{y_2} \quad \beta_{x_3} \quad \beta_{y_3} \rangle^T \tag{51}$$

Transverse shear strain field in parametric space is

$$\begin{Bmatrix} \underline{\gamma}_\xi \\ \underline{\gamma}_\eta \end{Bmatrix} = \begin{Bmatrix} w_{,\xi} + \beta_\xi \\ w_{,\eta} + \beta_\eta \end{Bmatrix} = \begin{Bmatrix} w_2 - w_1 + \beta_\xi \\ w_3 - w_1 + \beta_\eta \end{Bmatrix} \tag{52}$$

Then, substituting (49) into (52) we get the expression of shear strain in parametric space

$$\begin{gathered} \begin{Bmatrix} \underline{\gamma}_\xi \\ \underline{\gamma}_\eta \end{Bmatrix} = \left[B_{s_\xi}\right]\{u_n\} \\ \left[B_{s_\xi}\right] = \left[\left[B_{s_{\xi 1}}\right] \quad \left[B_{s_{\xi 2}}\right] \quad \left[B_{s_{\xi 3}}\right]\right] \\ \left[B_{s_{\xi 1}}\right] = \frac{1}{2}\begin{bmatrix} -2 & \left(x_{21} + x_{32}\,\eta\right) & \left(y_{21} + y_{32}\,\eta\right) \\ -2 & -\left(x_{13} + x_{32}\,\xi\right) & -\left(y_{13} + y_{32}\,\xi\right) \end{bmatrix} \\ \left[B_{s_{\xi 2}}\right] = \frac{1}{2}\begin{bmatrix} 2 & \left(x_{21} + x_{13}\,\eta\right) & \left(y_{21} + y_{13}\,\eta\right) \\ 0 & -x_{13}\xi & -y_{13}\xi \end{bmatrix} \\ \left[B_{s_{\xi 3}}\right] = \frac{1}{2}\begin{bmatrix} 0 & x_{21}\eta & y_{21}\eta \\ 2 & -\left(x_{13} + x_{21}\,\xi\right) & -\left(y_{13} + y_{21}\,\xi\right) \end{bmatrix} \end{gathered} \tag{53}$$

Transverse shear strain field in Cartesian system is

$$\{\underline{\gamma}\} = \begin{Bmatrix} \underline{\gamma}_x \\ \underline{\gamma}_y \end{Bmatrix} = [j] \begin{Bmatrix} \underline{\gamma}_\xi \\ \underline{\gamma}_\eta \end{Bmatrix} \tag{54}$$

Where $[j]$ is the inverse of the Jacobian matrix.

From Eq. (53) and Eq. (54), we obtain

$$\{\underline{\gamma}\} = \begin{Bmatrix} \underline{\gamma}_x \\ \underline{\gamma}_y \end{Bmatrix} = [B_s]\{u_n\} \quad ; \quad [B_s] = [j]\left[B_{s_\xi}\right] \tag{55}$$

The shear stiffness for MITC3 is calculated using three-points of Hammer integration (Jeon *et al*. 2015).

It is interesting to note that the shear strain matrix $[B_s]$

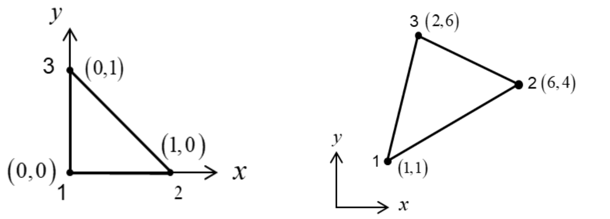

(a) Single Isosceles triangle (b) Single Arbitrary triangle

Fig. 6 Single triangular element test

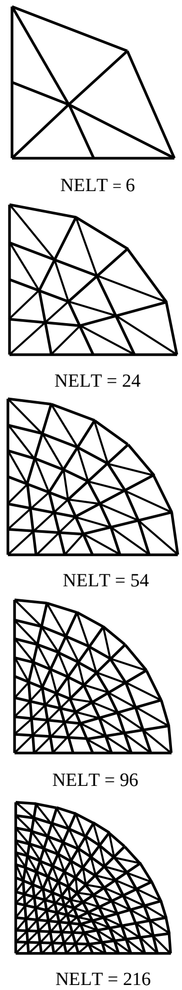

Fig. 7 A quarter of Circular plate with different number of elements (NELT)

for MITC3 element in the Eq. (55) is the same with the shear strain matrix $[B_s]$ for T3γ_s element in Eq. (23). The shear strain matrix $[B_s]$ for T3γ_s and MITC3 elements is finally given by

$$\begin{gathered} [B_s] = \left[\left[B_{s_1}\right] \quad \left[B_{s_2}\right] \quad \left[B_{s_3}\right]\right] \\ \left[B_{s_1}\right] = \frac{1}{4A}\begin{bmatrix} -y_{13} & -y_{21} \\ x_{13} & x_{21} \end{bmatrix}\begin{bmatrix} -2 & \left(x_{21} + x_{32}\,\eta\right) & \left(y_{21} + y_{32}\,\eta\right) \\ -2 & -\left(x_{13} + x_{32}\,\xi\right) & -\left(y_{13} + y_{32}\,\xi\right) \end{bmatrix} \\ \left[B_{s_2}\right] = \frac{1}{4A}\begin{bmatrix} -y_{13} & -y_{21} \\ x_{13} & x_{21} \end{bmatrix}\begin{bmatrix} 2 & \left(x_{21} + x_{13}\,\eta\right) & \left(y_{21} + y_{13}\,\eta\right) \\ 0 & -x_{13}\xi & -y_{13}\xi \end{bmatrix} \\ \left[B_{s_3}\right] = \frac{1}{4A}\begin{bmatrix} -y_{13} & -y_{21} \\ x_{13} & x_{21} \end{bmatrix}\begin{bmatrix} 0 & x_{21}\eta & y_{21}\eta \\ 2 & -\left(x_{13} + x_{21}\,\xi\right) & -\left(y_{13} + y_{21}\,\xi\right) \end{bmatrix} \end{gathered} \tag{56}$$

Table 1 Exact solution for circular plate (Batoz and Dhatt 1990)

Simply supported	Clamped
$w=\frac{f_z R^4}{64D_b}\left(1-\xi^2\right)\left(\frac{(6+2\upsilon)}{(1+\upsilon)}-\left(1+\xi^2\right)+\frac{8(h/R)^2}{3k(1-\upsilon)}\right)$	$w=\frac{f_z R^4}{64D_b}\left(1-\xi^2\right)\left(\left(1+\xi^2\right)+\frac{8(h/R)^2}{3k(1-\upsilon)}\right)$
$M_r=\frac{f_z R^2}{16}(3+\upsilon)\left(1-\xi^2\right)\;\;;\;\;\xi=\frac{r}{R}$	$M_r=\frac{f_z R^2}{16}(1+\upsilon)\left(1-\frac{(3+\upsilon)}{(1+\upsilon)}\xi^2\right)$

Table 2 Displacements $\underline{w}_c$ for the simply and clamped of circular plate under uniform loading

$\underline{w}_c$		Simply supported				Clamped			
		R/h = 500	R/h = 50	R/h = 5	R/h = 2.5	R/h = 500	R/h = 50	R/h = 5	R/h = 2.5
T3γ_s	NELT = 6	44.091	45.998	55.854	64.367	0.008	0.717	11.279	20.210
	NELT = 24	51.134	58.328	63.728	72.312	0.183	7.628	16.683	25.300
	NELT = 54	54.149	61.166	65.264	73.842	0.958	12.692	17.699	26.282
	NELT = 96	51.229	62.309	65.790	74.368	2.692	14.408	18.038	26.616
	NELT = 216	56.797	63.133	66.162	74.737	7.883	15.278	18.274	26.848
	NELT = 384	59.602	63.365	66.291	74.863	11.785	15.473	18.355	26.926
MITC3	NELT = 6	44.091	45.998	55.854	64.367	0.008	0.717	11.279	20.210
	NELT = 24	51.134	58.328	63.728	72.312	0.183	7.628	16.683	25.300
	NELT = 54	54.149	61.166	65.264	73.842	0.958	12.692	17.699	26.282
	NELT = 96	51.229	62.309	65.790	74.368	2.692	14.408	18.038	26.616
	NELT = 216	56.797	63.133	66.162	74.737	7.883	15.278	18.274	26.848
	NELT = 384	59.602	63.365	66.291	74.863	11.785	15.473	18.355	26.926
DKMT	NELT = 6	60.531	60.557	63.139	71.195	16.466	16.490	19.074	27.127
	NELT = 24	63.011	63.037	65.741	74.217	15.967	15.992	18.720	27.212
	NELT = 54	63.360	63.386	66.147	74.696	15.789	15.814	18.586	27.137
	NELT = 96	63.464	63.490	66.283	74.849	15.713	15.739	18.531	27.098
	NELT = 216	63.530	63.555	66.378	74.952	15.653	15.679	18.491	27.062
	NELT = 384	63.547	63.576	66.411	74.984	15.631	15.657	18.475	27.046
Exact solution		63.702	63.730	66.559	75.136	15.625	15.654	18.482	27.054

5. Numerical analysis

5.1 Single element test

To compare MITC3 and T3γ_s elements, we will compare the results of the formulation of both elements for simple cases. Two single triangles cases have been chosen (Fig. 6). As bending strain matrices for both elements are obtained in the same way, we will only compare the impact of the shear strain matrices.

If we substitute the coordinates of isosceles and arbitrary triangles (Fig. 6) into Eqs. (23) and (55) we obtain the same shear strain matrices $[B_s]$, which leads to the same shear stiffness.

5.2 Convergence tests

Next, we will consider a quarter of circular plate (Fig. 7) under uniform loading f_z for convergence studies. Because of symmetry, only one quarter of circular plate is evaluated and divided in 3 zones. For each zone we consider N×N×2 elements. Two cases will be studied with number of elements (NELT) of 6, 24, 54, 96, 216 and 384. R = 5; h =0.01, 0.1, 1, 2; R/h = 500, 50, 5, 2.5; E = 10.92; Poisson's ratio = 0.3; and uniform loading f_z = 1.

In the first case, the perimeter edge is simply supported (soft simply supported), while in the second it is fixed. The analytical solution is given in Table 1.

We observe the displacement at the centre of the plate (w_c). The numerical results for T3γ_s and for MITC3 are compared with DKMT element and the exact results, as

Table 3 Moment M_r at the center of circular plate for simply and clamped under uniform loading

		Simply supported				Clamped			
		R/h = 500	R/h = 50	R/h = 5	R/h = 2.5	R/h = 500	R/h = 50	R/h = 5	R/h = 2.5
T3γ_s	NELT = 6	2.868	3.124	4.118	4.182	0.001	0.097	1.207	1.318
	NELT = 24	3.150	4.524	4.899	4.906	0.031	1.099	1.842	1.852
	NELT = 54	3.368	4.870	5.044	5.045	0.110	1.687	1.951	1.953
	NELT = 96	3.117	5.018	5.094	5.094	0.273	1.897	1.988	1.989
	NELT = 216	4.219	5.109	5.128	5.128	0.900	1.996	2.013	2.013
	NELT = 384	4.690	5.132	5.139	5.140	1.490	2.016	2.021	2.021
MITC3	NELT = 6	2.868	3.124	4.118	4.182	0.001	0.097	1.207	1.318
	NELT = 24	3.150	4.524	4.899	4.906	0.031	1.099	1.842	1.852
	NELT = 54	3.368	4.870	5.044	5.045	0.110	1.687	1.951	1.953
	NELT = 96	3.117	5.018	5.094	5.094	0.273	1.897	1.988	1.989
	NELT = 216	4.219	5.109	5.128	5.128	0.900	1.996	2.013	2.013
	NELT = 384	4.690	5.132	5.139	5.140	1.490	2.016	2.021	2.021
DKMT	NELT = 6	5.261	5.262	5.333	5.417	2.400	2.401	2.472	2.554
	NELT = 24	5.220	5.221	5.267	5.290	2.163	2.164	2.212	2.235
	NELT = 54	5.194	5.195	5.225	5.233	2.101	2.102	2.133	2.141
	NELT = 96	5.179	5.181	5.201	5.205	2.074	2.075	2.096	2.099
	NELT = 216	5.166	5.167	5.178	5.179	2.052	2.053	2.064	2.065
	NELT = 384	5.160	5.161	5.169	5.169	2.043	2.044	2.050	2.051
Exact solution		5.156	5.156	5.156	5.156	2.031	2.031	2.031	2.031

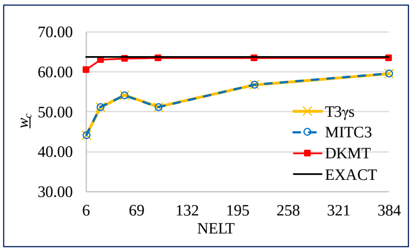

(a) Simply supported

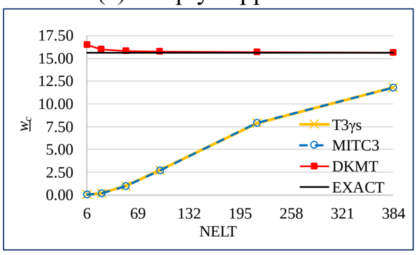

(b) Clamped

Fig. 8 Displacement $\underline{w}_c$ of circular plate for simply and clamped with R/h = 500

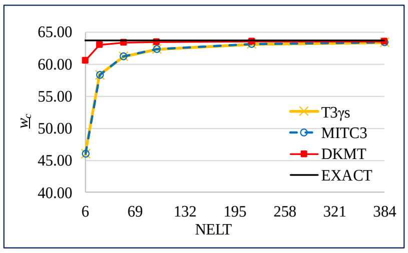

(a) Simply supported

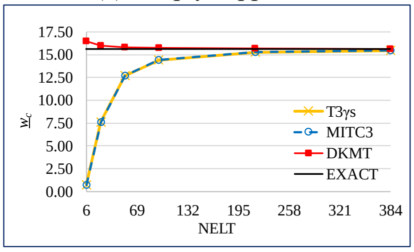

(b) Clamped

Fig. 9 Displacement $\underline{w}_c$ of circular plate for simply and clamped with R/h = 50

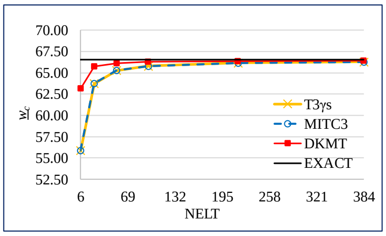

(a) Simply supported

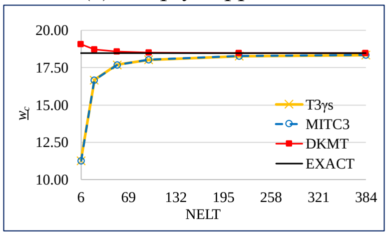

(b) Clamped

Fig. 10 Displacement $\underline{w}_c$ of circular plate for simply and clamped with R/h = 5

shown in Table 2 for normalized vertical displacement $\underline{w}_c = w_c \times D_b \times 10^3 \big/ f_z R^4$ and in Table 3 for bending moment M_r at the centre.

As we can see from Tables 2 and 3, both T3γ_s and MITC3 show exactly the same results. Evidently, although based on different formulation ideas, both elements lead to the same stiffness matrix.

Figs. 8-11 show the comparative results of T3γ_s, MITC3 and DKMT elements for R/h, i.e., R/h = 500, 50, 5 and 2.5 for vertical displacement at the center of the plate. Figs. 12-15 show comparative results of moment M_r at the center of the plate.

For thin plate (R/h = 500), we observe the poor behavior of MITC3 (T3γ_s) due to shear locking problem and excellent performance is shown for DKMT ≈ DKT gives the better results. For R/h = 50, we observe that less shear locking using MITC3 and T3γ_s, compared with previous

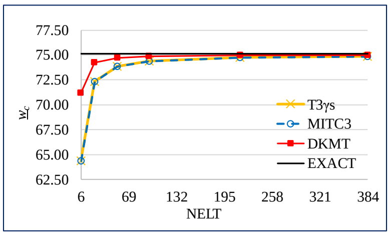

(a) Simply supported

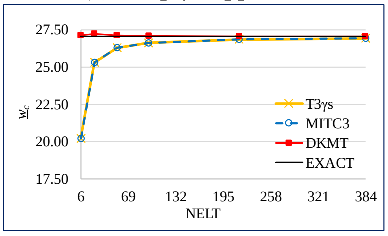

(b) Clamped

Fig. 11 Displacement $\underline{w}_c$ of circular plate for simply and clamped with R/h = 2.5

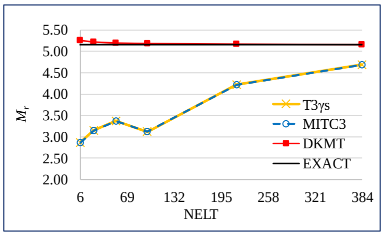

(a) Simply supported

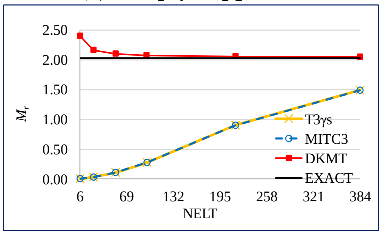

(b) Clamped

Fig. 12 Moment M_r at the center of circular plate for simply and clamped with R/h = 500

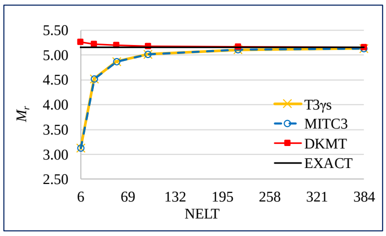

(a) Simply supported

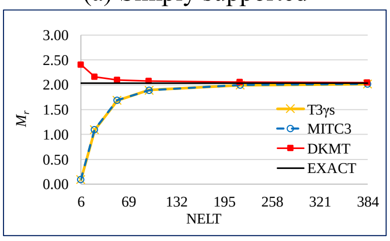

(b) Clamped

Fig. 13 Moment M_r at the center of circular plate for simply and clamped with R/h = 50

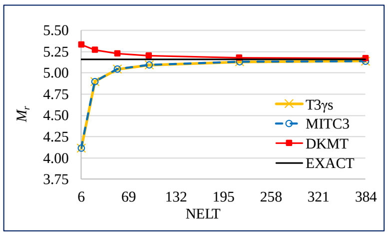

(a) Simply supported

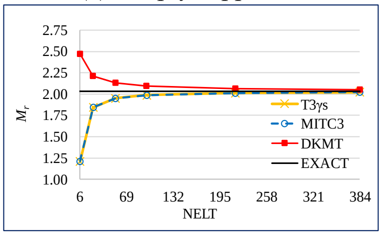

(b) Clamped

Fig. 14 Moment M_r at the center of circular plate for simply and clamped with R/h = 5

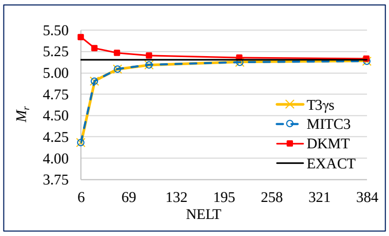

(a) Simply supported

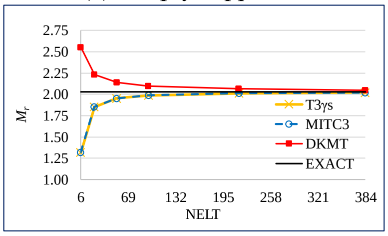

(b) Clamped

Fig. 15 Moment M_r at the center of circular plate for simply and clamped with R/h = 2.5

plate cases (R/h = 500). We remark the overall best performances and gives good convergence behavior to the exact solution of DKMT, T3γ_s and MITC3 for R/h = 2.5.

6. Conclusions

The paper includes detailed formulation aspects of the stiffness matrix of three triangular plate bending elements with 3 *dof* per node, based on the first order Reissner-Mindlin theory. The three elements T3γ_s, DKMT and MITC3, have been published in 1982, 1993 and 2004.

The present paper is written in order to understand the differences and complementarities, using a unified notation and similar assumed shear strain constraints on element sides.

Although T3γ_s and MITC3 elements are obtained considering two different methods, the formulation of these two elements are actually identical, which is proved by the same bending strain and shear strain matrices. The paper shows that for thin plates DKMT should converge to DKT without shear locking. On the other end for extremely thick plates the formulation of DKMT is such that $\text{DKMT} \approx \text{T3}\gamma_s(\text{MITC3})$. The results of numerical tests confirm that the three elements show a good convergence towards the exact solution. However, better results for displacement and stresses are obtained using the DKMT element due to incomplete quadratic interpolation of the rotations.

Acknowledgements

The authors gratefully acknowledge financial support from Universitas Indonesia through the PITTA program (2454/UN2.R3.1/HKP.05.00/2018).

References

Katili, I., Batoz, J.L., Maknun, I.J., Hamdouni, A. and Millet, O. (2014), “The development of DKMQ plate bending element for thick to thin shell analysis based on Naghdi/Reissner/Mindlin shell theory”, *Fin. Elem. Anal. Des.*, **100**, 12-27.

Katili, I., Maknun, I.J., Millet, O. and Hamdouni, A. (2015), “Application of DKMQ element for composite plate bending structures”, *Compos. Struct.*, **132**, 166-174.

Mahjudin, M., Lardeur, P., Druesne, F. and Katili, I. (2016), “Stochastic finite element analysis of plates with the certain generalized stresses method”, *Struct. Saf.*, **61**, 12-21.

Maknun, I.J., Katili, I., Millet, O. and Hamdouni, A. (2016), “Application of DKMQ element for a twist of thin-walled beams: Comparison with Vlasov theory”, *Int. J. Comput. Meth. Eng. Sci. Mech.*, **17**, 391-400.

Wong, F.T., Richard, A. and Katili, I. (2017), “Development of the DKMQ element for buckling analysis of shear-deformable plate bending”, *Proc. Eng.*, **171**, 805-812.

Katili, I., Batoz, J.L., Maknun, I.J. and Lardeur, P. (2018), “A comparative formulation of DKMQ, DSQ and MITC4 quadrilateral plate elements with new numerical results based on s-norm tests”, *Comput. Struct.*, **204**, 48-64.

Katili, I., Maknun, I.J., Batoz, J.L. and Ibrahimbegović, A. (2018), “Shear deformable shell element DKMQ24 for composite structures”, *Compos. Struct.*, **202**, 182-200.

Katili, I., Maknun, I.J., Batoz, J.L. and Katili, A.M. (2018), “Asymptotic equivalence of DKMT and MITC3 elements for thick composite plates”, *Compos. Struct.*, **206**, 363-379.

Ko, Y., Lee, P.S. and Bathe, K.J. (2017), “A new MITC4+ shell element”, *Comput. Struct.*, **182**, 404-418.

Banh, T.T. and Lee, D. (2018), “Multi-material topology optimization of Reissner-Mindlin plates using MITC4”, *Steel Compos. Struct.*, **27**, 27-33.

Hughes, T.J.R. and Tezduyar, T.E. (1981), “Finite elements based upon Mindlin plate theory with particular reference to the four-node bilinear isoparametric element”, *Trans. ASME J. App. Mech.*, **48**(3), 587-596.

MacNeal, R.H. (1982), “Derivation of element stiffness matrices by assumed strain distributions”, *Nucl. Eng. Des.*, **70**(1), 3-12.

Hughes, T.J.R. and Taylor, R.L. (1982), *The Linear Triangle Bending Elements*, The Mathematics of Finite Element and Application IV, MAFELAP, Academic Press, London, U.K.

Ayad, R., Batoz, J.L., Dhatt, G. and Katili, I. (1992), *A Study of*

Recent Triangular Elements for Thin and Thick Plates, Elsevier.

Batoz, J.L., Bathe, K.J. and Ho, L.W. (1980), "A study of three-node triangular plate bending elements", *Int. J. Numer. Meth. Eng.*, **15**(12), 1771-1812.

Batoz, J.L. and Lardeur, P. (1989), "A discrete shear triangular nine dof element for the analysis of thick to very thin plates", *Int. J. Numer. Meth. Eng.*, **28**(3), 533-560.

Katili, I. (1993), "A new discrete Kirchhoff-Mindlin element based on Mindlin-Reissner plate theory and assumed shear strain fields-part I: An extended DKT element for thick-plate bending analysis", *Int. J. Numer. Meth. Eng.*, **36**(11), 1859-1883.

Lee, P.S. and Bathe, K.J. (2004), "Development of MITC isotropic triangular shell finite elements", *Comput. Struct.*, **82**(11-12), 945-962.

Lee, P.S., Noh, H.C. and Bathe, K.J. (2007), "Insight into 3-node triangular shell finite elements: The effect of element isotropy and mesh pattern", *Comput. Struct.*, **85**(7-8), 404-418.

Lee, Y., Yoon, K. and Lee, P.S. (2012), "Improving the MITC3 shell finite element by using the Hellinger-Reissner principle", *Comput. Struct.*, **110-111**, 93-106.

Lee, Y., Lee, P.S. and Bathe, K.J. (2014), "The MITC3+ shell element and its performance", *Comput. Struct.*, **138**, 12-23.

Jeon, H.M., Lee, Y., Lee, P.S. and Bathe, K.J. (2015), "The MITC3+ shell element in geometric nonlinear analysis", *Comput. Struct.*, **146**, 91-104.

Ko, Y., Lee, Y., Lee, P.S. and Bathe, K.J. (2017), "Performance of MITC3+ and MITC4+ shell elements in widely-used benchmark problems", *Comput. Struct.*, **193**, 187-206.

Batoz, J.L. and Dhatt, G. (1990), *Modélisation des Structures par Elément Finis, Poutres et Plaques*, Hermes, Paris, France.

CC